International Journal of Thermophysics, Vol. 19, No. 4, 1998

Surface Adsorption in a Surfactant/Clay Mineral Solution[1]

H. J. M. Hanley,[2,3] C. D. Muzny,[2] and B. D. Butler[2]

The complexes formed in aqueous mixture suspensions of the synthetic clay mineral Laponite and cetyltrimethylammonium bromide (CTAB) have been investigated by small-angle neutron scattering (SANS). All suspensions were prepared with a constant initial concentration of Laponite, but the amount of CTAB was varied. The SANS intensity patterns verify that suspended Laponite in dilute suspension is in the form of disks of diameter ~30 nm and thickness ~1 nm. SANS indicates that this disk morphology, with the same diameter but with a thickness of about 4 nm, is retained for the suspended complexes, even if the CTAB in the aqueous medium is in considerable excess. SANS and chemical analysis show that a complex must adsorb CTAB to an amount corresponding to at least two multiples of the clay's cation exchange capacity to be dispersed. The amount of CTAB adsorbed as a function of CTAB in the precursor solution is discussed. We also report the effect the presence of clay on CTAB micelle formation as a function of CTAB concentration.

KEY WORDS: adsorption; cation exchange capacity; clay mineral; complex; CTAB; Laponite; micelle; small angle neutron scattering (SANS); suspensions.

1. INTRODUCTION

We have recently reported [1] some small-angle neutron scattering results on complexes prepared in aqueous suspension by adding the cationic surfactant cetyltrimethylammonium bromide (CTAB), $CH_3(CH_2)_{15}(CH_3)_2N^+Br^-$, to a dilute suspension of the synthetic clay mineral, Laponite. Complexes are formed when the CTAB is mixed with an aqueous medium of the dispersed

---

[1] Paper presented at the Thirteenth Symposium on Thermophysical Properties, June 22-27, 1997, Boulder, Colorado, U.S.A.

[2] Physical and Chemical Properties Division, National Institute of Standards and Technology, 325 Broadway, Boulder, Colorado 80303, U.S.A.

[3] To whom correspondence should be addressed.

0195-928X/98/0700-1155$15.00/0

clay because the sodium ions exchange with the CTA^+ ions. If, however, the amount of CTAB initially in solution is such that a roughly complete exchange could occur—that is, the clay's cation exchange capacity (CEC) is saturated—the platelet complexes become hydrophobic and aggregate face to face. Sorption of surfactant over and above the CEC, however, introduces a surface charge and causes the aggregates partially to (re)disperse: it is a well-known and accepted assumption that the coated clay redisperses because excess surfactant molecules orient themselves with their head groups away from the clay surface, forming a charged micelle-like complex in the aqueous solvent [2]. These clay/CTAB dispersions are the systems of interest to us. We were particularly interested to find out exactly what surface excess of CTAB is needed to cause redispersion, and whether this surface excess is a function of the amount of CTAB added to the precursor (initial) solution. Most of the stable complexes are dispersed in solutions that contained concentrations of CTAB well above the critical micelle concentration (CMC), and it was interesting to see what effect the clay had on micelle formation.

2. EXPERIMENTAL

2.1. Solution Preparation and Analysis

The properties of Laponite have been documented by the manufacturers [3] and by other investigators [4]. Laponite has a basic unit made up of a layered hydrous magnesium silicate platelet of diameter 25 to 30 nm, with a thickness of approximately 1 nm, and has the molecular formula approximated by $Si_8[Mg_{5.54}Li_{0.46}H_4O_{24}]^{0.57-}Na^+_{0.57}$. Here the cation exchange capacity is taken to be 0.745 $\text{mequiv} \cdot g^{-1}$ and the density is taken to be $2.53\ g \cdot cm^{-3}$ [4].

A clay stock solution was prepared by dispersing 1.0 % by mass of clay in HPLC grade H_2O and stirring for several hours until clear. All complexes were prepared from the stock by mixing a given volume with an equal volume of an appropriate aqueous solution of CTAB. Since the mixing caused aggregation, the mixtures were further stirred, then centrifuged at $19{,}600\ m \cdot s^{-2}$ for 30 min. The supernatants were taken as the samples for study and analyzed chemically for sodium by flame emission spectroscopy, for silicon and magnesium by atomic absorption spectroscopy, and for bromine by ion chromatography. The various supernatants are labeled in terms of the amount of CTAB present in the precentrifuged mixture with respect to the clay CEC, given the initial clay concentration of $5\ g \cdot L^{-1}$. For example, the sample labeled "1:1" was prepared by mixing an aqueous 3.75mM CTAB solution—corresponding to enough CTAB to effect one complete exchange between the Na^+ and the CTA^+ ion—with an equal volume of the stock clay solution. The other samples corresponded to precentrifuged CTAB/clay ratios designated 1/4:1, 1/2:1, 2:1, 3:1, 4:1, 5:1, 7:1, 10:1, and 13:1. All samples were investigated at temperatures between 298 and 303 K, temperatures above their estimated Krafft points.

Three equivalent aqueous solutions were prepared for the SANS experiments: in 100% H_2O, in 100% D_2O, and in a 50% H_2O/D_2O mixture. These varied solvents were required to contrast match the scattered length densities.

2.2. Neutron Scattering

Neutron scattering intensities $I(q)$ from the clay solution and complex solutions were measured as a function of the scattered wave vector q, where $q = 4\pi \sin(\theta/2)/\lambda$, with λ the incident neutron wavelength and θ the angle of scatter. The solutions were loaded in 1-mm gap thickness quartz cells and placed in the beam of the 30-m SANS NG7 spectrometer of the NIST Center for Neutron Research configured with an incident neutron wavelength $\lambda = 0.6$ nm and sample-detector distances of 13 and 3 m, with a 25-cm detector offset. The wave vector range for these configurations was $0.03 < q < 1.2\ \text{nm}^{-1}$. Scattered neutrons were detected on the instrument's 2D position-sensitive detector. The measured counts were azimuthally averaged, corrected for empty cell and solvent scattering, and placed on an absolute scale by normalizing to the intensity obtained from a water standard.

3. RESULTS

3.1. Chemical Analysis

Table I lists the results of the systems we were able to analyze. Listed are the sodium and bromine contents of the supernatants and the mass fractions (calculated from the silicon and magnesium supernatant content) of the clay in suspension and, by inference, as a precipitate. The masses are estimated to be accurate within 10% for the sodium, 6% for silicon, and 5% for bromine. The entries under the column designated CECP denote the CTAB/clay ratio of the precipitate, evaluated in terms of multiples of the CEC. This ratio is evaluated as follows: consider, for example, the 5:1 system. The initial mixture contained $18.73\ \text{mmol} \cdot \text{L}^{-1}$ of CTAB (or $1496\ \text{mg} \cdot \text{L}^{-1}$ of bromine) to correspond to five multiples of the cation exchange capacity. The analysis indicates that $848\ \text{mg} \cdot \text{L}^{-1}$ of bromine is left in the supernatant. Hence, $8\ \text{mmol} \cdot \text{L}^{-1}$ of CTAB must be associated

Table I. Composition of the Clay Complex Precipitates and Supernatants

Mixture[a]	Sodium in supernatant ($mg \cdot L^{-1}$)	Bromine in supernatant ($mg \cdot L^{-1}$)	Fraction clay precipitated	CECP
1/5:1[b]	101	55	0.29	$\leqslant$1:1
1/4:1	90	72	0.30	$\leqslant$1:1
1/2:1	85	140	0.62	$\leqslant$1:1
3:1	95	501	0.77	2.5:1
4:1	95	713	0.79	3:1
5:1	88	848	0.77	4:1
13:1	92	3160	0.76	4:1

[a] The label denotes the precentrifuged mixture CTAB/clay ratio, expressed as the amount of CTAB with respect to the cation exchange capacity (see text); CECP denotes the CTAB/clay ratio associated with the precipitate. Not all the samples studied by SANS were analyzed.
[b] From Ref. 1.

with the precipitate. The amount, however, of CTAB needed to reach the CEC is 2.9 $mmol \cdot L^{-1}$, given that the fraction 0.77 of the initial 5 $g \cdot L^{-1}$ of clay has been precipitated; whence CECP $\sim$3. The sodium and bromine analyses confirm, however, that CTAB is bonded by cation exchange to the clay. The bromine from that layer is released to solution. Hence, the total cation exchange multiple is $3 + 1$, or $CECP = 4$. We do not list this ratio for a 1:1 and a 2:1 system because the chemical analysis indicated that no solid was present in the supernatant, confirmed by SANS (see the discussion below) and light scattering [1].

The sodium is either released to the supernatant by the cation exchange or associated with dispersed clay. We have, however, argued in Ref. 1 that all the sodium in the liquids for samples designated 1:1 or greater must arise from the cation exchange: in other words, the cation exchange is complete. In this context, it is interesting to note that the analysis conveys that the fraction of clay precipitated from samples 1/5:1, 1/4:1, and 1/2:1 is roughly equal to the precentrifuged CTAB/clay ratio. Recalling that the precipitation occurs because the surfactant molecular chains are hydrophobic, we conclude that the CTAB prefers to saturate a fraction of the clay platelets rather than cover all of them more or less uniformly. This conclusion is supported in Ref. 1

3.2. Small-Angle Neutron Scattering

We write down the expressions needed to interpret the SANS results with minimal discussion [5]. The coherent contribution to the scattered intensity $I(q)$ from a monodisperse suspension of N particles in volume V (i.e., at density $n = N/V$) is proportional to the differential cross section per unit volume of the sample $d\Sigma/d\Omega$ (cm^{-1}):

$$d\Sigma/d\Omega = (N/V)\,|F(\mathbf{q})|^2\,S(\mathbf{q}) \tag{1}$$

This equation is written in terms of a single particle form factor,

$$F(\mathbf{q}) = \sum_j b_j \exp(i\mathbf{q}\cdot\mathbf{X}_j) \tag{2}$$

where $\mathbf{X}_j$ is the position of atomic nucleus j, with neutron scattering length b_j, and the structure factor

$$S(\mathbf{q}) = \frac{1}{N}\left\langle \sum_i \sum_{i'} \exp[i\mathbf{q}\cdot(\mathbf{R}_i - \mathbf{R}_{i'})]\right\rangle \tag{3}$$

where $\mathbf{R}_i$ is the vector for the center of mass of particle i.

Experimentally, scattering from a species is measured with respect to the scattering length density of the medium ρ_m and Eq. (2) becomes

$$F(\mathbf{q}) = \int dr[\rho(\mathbf{r}) - \rho_m]\,\exp(i\mathbf{q}\cdot\mathbf{r}) \tag{4}$$

Here, a particle or molecular scattering length density is defined operationally by $\rho = \rho_\mathrm{mol}\sum b_j N(j)$, where ρ_mol is the molecular density and $N(j)$ is the number of nuclei of type j in a particle; ρ_m is the weighted number fraction of the scattering length densities of the molecular components of the medium.

The working equation for the scattered intensity from an noninteracting system can be written in terms of the volume fraction ϕ, where $\phi = (N/V)\,V_\mathrm{p}$, with V_p the volume of the particle:

$$I(q) = A\phi V_\mathrm{p}(\rho - \rho_\mathrm{m})^2\,P(q) \tag{5}$$

where A is an apparatus constant. The term $P(q)$ is the square of the orientationally averaged $F(\mathbf{q})$ written in dimensionless form. For a sphere of radius R [5, 6],

$$P(q) = [3(\sin qR - qR\cos qR)/(qR)^3]^2 \tag{6}$$

and for a disk of radius R and height $2H$ [6],

$$P(q) = 4\int_0^{\pi/2}\left(\frac{\sin^2(qH\cos\beta)}{(qH)^2\cos^2\beta}\right)\frac{J_1^2(qR\sin\beta)}{(qR)^2\sin^2\beta}\sin\beta\,d\beta \tag{7}$$

where J_1 is the first integer-order Bessel function and β is the angle between $\mathbf{q}$ and the major axis of the disk. Equation (7) implies that a plot of log(I) versus log(q) from a system of noninteracting disk will have a slope of -2 for $qR > 2$ provided that $qH \ll 1$.

In our work, the scatterers are either the clay platelets for which the surface sodium ions have been replaced by an organic interface, or free CTAB micelles which can be treated as a center of hydrophobic tails and a surface of nitrogen head groups [7]. In other words, both particle types can be considered as made up of a central core and a surface coating. In general, if the core has a characteristic scattering length density ρ_1 and the surface has a characteristic scattering length density ρ_2, the scattered intensity from a system of isolated particles [that is, with $S(q) = 1$] is of the form

$$I(q) \sim \{(\rho_2 - \rho_m)[V_T P_T(q) - V_1 P_1(q)] + (\rho_1 - \rho_m) V_1 P_1(q)\}^2 \quad (8)$$

where V_1 is the volume of the core, and V_T is the total volume of the particle.

3.2.1. CTAB Adsorption

Figure 1 displays a typical result from the SANS experiments. It shows the measured absolute cross sections from a 5:1 supernatant [1] with three aqueous media: D_2O (top curve), a 50 % by volume D_2O/H_2O mixture (middle curve), and H_2O (bottom curve). Inspection of Eq. (8) indicates that if $\rho_m \equiv \rho_{H_2O}$, the scattering will be essentially that from a pure clay suspension. If, however, $\rho_m \equiv \rho_{H_2O/D_2O}$, scattering from the CTAB dominates because the clay scattering has been nearly contrasted out, and if $\rho_m \equiv \rho_{D_2O}$, the scattering will have components from both species. Fits of Eq. (7) to the pure clay intensity curves, for this example and the other supernatants, are consistent with a clay platelet radius $R = 15 \pm 1$ nm and the half-height $H = 0.55 \pm 0.3$ nm—values slightly larger but close to those obtained by others [4]. The power-law slope of the clay curves in the range $0.15 < q < 0.4\ \text{nm}^{-1}$ from all the supernatants with solids present was ~ -2.1: the signature expected of a disk.

4. DISCUSSION AND CONCLUSION

We can infer three main observations from Fig. 1 and from its equivalents for the other systems.

1. The D_2O data (top curve in Fig. 1) and the D_2O/H_2O data (middle curve in Fig. 1) are consistent with scattering patterns from a disk:

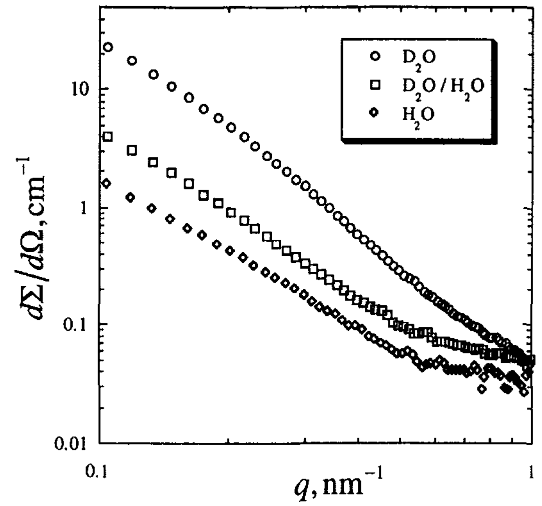

Fig. 1. Absolute SANS scattering cross sections from the supernatant designated 5:1. The various aqueous media were selected to contrast the constituents of the complex: the lower curve represents scattering from the clay, the middle curve from the CTAB, and the upper curve from the complex.

that the curves are not parallel with the bottom curve for pure Laponite can be explained by the fact that the disk appears thicker in the D_2O media. We thus conclude that the Laponite disk geometry is preserved in the clay/surfactant complex.

2. The displacements in intensity extrapolated to zero *q*[1] give an estimate of the amount of CTAB attached to the clay. For the 5:1 system, we estimated that four CEC multiples of CTAB were on the clay platelet face, a conclusion consistent with the chemical analysis result that CECP = 4 (Table I).

3. Figure 2 is a plot of the displacement between the D_2O runs and the H_2O runs for all the supernatants. A difference is defined by [intensity (D_2O medium) − intensity (H_2O medium)], but the H_2O data have been scaled because the amount of solid varied from one supernatant to another. The difference curves for the 5:1, 7:1, 10:1, and 13:1 systems (and also for a 20:1 system, not shown here) can essentially be superimposed. In other words, the amount of CTAB adsorbed must reach a saturation value of about 4 CEC multiples. We also note that the CEC multiples inferred from the curves for the 3:1 and 4:1 complexes with respect to the curve for

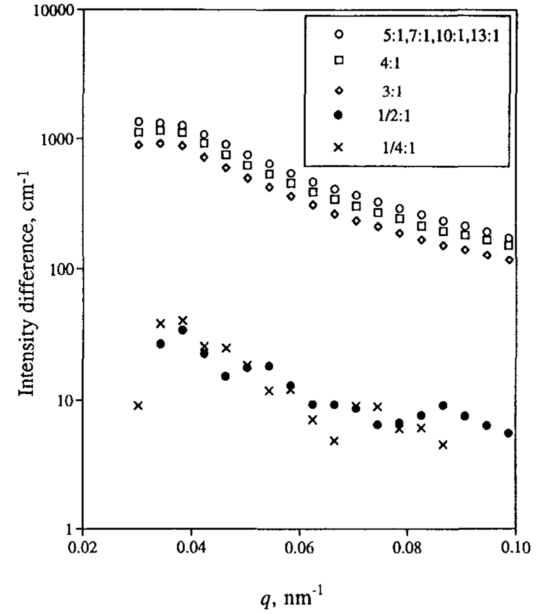

Fig. 2. Plot of the scaled displacement [intensity (D_2O medium) − intensity (H_2O medium)]. This displacement corresponds to the difference between the intensity from CTAB-coated Laponite and the intensity from pure Laponite (see text). The curves for the 5:1, 7:1, 10:1, and 13:1 systems are essentially superimposible. The 5:1 result indicates a CTAB coverage of 4 CEC multiples. The coverage for the other systems scales accordingly.

the 5:1 system are 2.7 and 3.3, respectively. This SANS result is in excellent agreement with the result obtained from the chemical analysis (Table I).

We end with a comment on micelle formation in a system with clay present. We might have expected to see evidence of micelle formation since the SANS intensities were measured from complexes prepared from CTAB solutions in which the concentration of CTAB was (with the possible exception of the 1/4:1 mixture) well above the critical micelle concentration of 0.82 mmol · L^{-1} in D_2O[7]. Inspection, however, of the curve in Fig. 1 for the 5:1 supernatant, and the curves for the 3:1, 4:1, and 7:1 mixtures in Fig. 2, gives no hint of a peak that would result from micelle–micelle interactions. To reinforce this statement we have plotted data for the 5:1 system at higher values of q in Fig. 3. For comparison, a clay-free CTAB solution was prepared with a concentration of CTAB slightly in excess of that in the 5:1 supernatant and designated 5:0. This

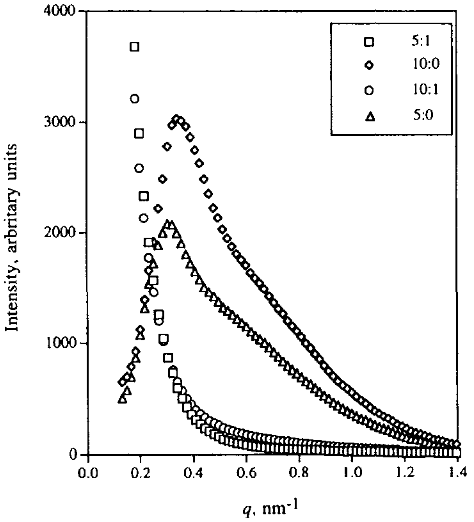

Fig. 3. Variation of the intensities of the complex supernatants with respect to their corresponding micellar solutions.

solution contains micelles and the intensity pattern is shown in Fig. 3. The curve displays a peak at about $q = 0.25$ nm^{-1}. Comparison between the 5:1 and the 5:0 curves indicates clearly that the presence of the clay in the 5:1 mixture has suppressed micelle formation in the CTAB solution above the complex. We, however, also plot in Fig. 3 the curve for the 10:1 supernatant, which shows a marked increase in scattered intensity for $q \geqslant 0.15$. This enhancement corresponds to an intensity peak observed from a clay-free CTAB solution designated 10:0. Undoubtedly, then, micelles can form in the 10:1 mixture. We plan to investigate the concept of micelle formation in the presence of a charged surface in general.

ACKNOWLEDGMENTS

This work was sponsored by the Air Force Office of Scientific Research, USAF, under Grant AFOSR-MIPR-94-0027. Some of the SANS data were taken on the 30-m spectrometer supported by the National Science Foundation under Agreement DMR-9423101. We thank the staff of the NIST Center for Neutron Research for their support and encouragement.

REFERENCES

1. H. J. M. Hanley, C. D. Muzny, and B. D. Butler. *Langmuir* **13**:5276 (1997).
2. For example, B. K. G. Theng, *Formation and Properties of Clay-Polymer Complexes* (Elsevier, Amsterdam, 1979); D. J. Greenland and J. P. Quirk, *Clays Clay Min.* **9**:484 (1962); P. Labbe and G. Reverdy, *Langmuir* **7**:2000 (1991).
3. *Laponite Technical Bulletin, L104/90/A*, Laporte Industries, UK. The name Laponite is used to identify the product. Endorsement by NIST is not implied.
4. For example, M. Morvan, D. Espinat, J. Lambard, and T. Zemb, *Colloids Surf. Pt. A* **82**:193 (1994); B. S. Neumann, and K. G. Sansom, *Israel J. Chem.* **8**:315 (1970); J. D. F. Ramsay, S. W. Swanton, and J. Bunce, *J. Chem. Soc. Faraday Trans.* **86**:3919 (1990).
5. For example, S.-H. Chen, and T. S. Lin, in *Methods in Experimental Physics, Vol. 23, Part B, Neutron Scattering*, D. L. Price and K. Skold, eds. (Academic Press, London, 1987); *Small Angle X-ray Scattering*, O. Glatter and O. Kratky, eds. (Academic Press, London, 1982).
6. A. Guinier and G. Fournet, *Small-Angle Scattering of X-Rays* (Wiley, New York, 1955).
7. S. S. Berr, E. Caponetti, J. S. Johnson, R. R. M. Jones, and L. J. Magid, *J. Phys. Chem.* **90**:5766 (1986).